Journal of Biosciences and Medicines, 2026, 14(2), 230-243
https://www.scirp.org/journal/jbm
ISSN Online: 2327-509X
ISSN Print: 2327-5081

miRNA-30b-5p Targets P4HA2 to Regulate Osteosarcoma Cell Proliferation, Invasion, Migration, and Apoptosis

Wusong Liu[1*], Wei Fu[1*], Tianyi Shen[1], Wenwen Tang[1,2], Changgong Lan[1,2#]

[1]School of Clinical Medicine, Youjiang Medical University for Nationalities, Baise, China
[2]The Affiliated Hospital of Youjiang Medical University for Nationalities, Baise, China
Email: #landlong120@sina.com

How to cite this paper: Liu, W.S., Fu, W., Shen, T.Y., Tang, W.W. and Lan, C.G. (2026) miRNA-30b-5p Targets P4HA2 to Regulate Osteosarcoma Cell Proliferation, Invasion, Migration, and Apoptosis. *Journal of Biosciences and Medicines*, **14**, 230-243.
https://doi.org/10.4236/jbm.2026.142017

Received: January 6, 2026
Accepted: February 3, 2026
Published: February 6, 2026

Abstract

Objective: This study aims to elucidate the mechanism by which the microRNA miR-30b-5p inhibits the proliferation, invasion, and migration of osteosarcoma cells while inducing apoptosis through the regulation of P4HA2. **Methods**: The MG63 osteosarcoma cell line was transfected with miR-NC and miR-30b-5p mimics to establish negative control and miR-30b-5p up-regulated expression models. Subsequently, various assays were conducted, including the CCK8 assay, Transwell assay, flow cytometry, dual luciferase reporter assay, real-time PCR (RT-PCR), and Western blot analysis. **Results:** Following the transfection of MG63 cells with miR-30b-5p mimics, the expression of miR-30b-5p was significantly up-regulated compared to the control group ($t = 77.53$, $p = 0.0002$). After transfecting the cells with miR-NC and miR-30b-5p mimics for 24, 48, and 72 hours, the CCK8 assay results indicated a marked reduction in proliferative ability relative to the control group (24 h: $t = 16$, $P < 0.001$; 48 h: $t = 5.318$, $P < 0.0001$; 72 h: $t = 10.58$, $P < 0.0001$). Additionally, the Transwell assay results demonstrated that the invasive ability of cells in the miR-30b-5p mimics group was significantly lower than that in the miR-NC group ($t = 8.92$, $P < 0.0001$), and the migration level was also significantly reduced ($t = 23$, $P < 0.0001$). Flow cytometry analysis revealed that the apoptosis level of MG63 cells in the miR-30b-5p mimics group was significantly increased compared to the miR-NC group ($t = 14.06$, $P = 0.0001$). Dual-luciferase reporter assay demonstrated that P4HA2 is a direct target molecule of miR-30b-5p. Furthermore, RT-PCR and Western blot experiments confirmed that the expression of P4HA2 in osteosarcoma cells was significantly down-regulated at both the mRNA and protein levels following miR-30b-5p transfection. In contrast, the expression of the pro-apoptotic protein BAX was ele-

*These authors share first authorship.
#Corresponding author.

vated, while the expression of the anti-apoptotic protein BCL-2 was decreased. **Conclusion:** miR-30b-5p plays a role in inhibiting the proliferation, invasion, and migration of osteosarcoma cells while also inducing apoptosis by targeting and down-regulating P4HA2 expression. However, the experiments were constrained, as they were validated in a single cell line and lacked the most direct evidence obtained through "functional recovery assays. experiments".

Keywords

Osteosarcoma, P4HA2, miR-30b-5p

1. Introduction

Osteosarcoma is the most prevalent primary bone tumor among children and adolescents, distinguished by its high malignancy, significant metastatic potential, and poor prognosis following metastasis [1] [2]. The complexity and instability of the osteosarcoma genome, coupled with a limited understanding of the precise mechanisms underlying its development, have hindered advancements in treatment [3]. Although numerous researchers are investigating the pathogenesis of osteosarcoma, the prognosis for patients with metastatic disease has not significantly improved, and novel therapeutic strategies are still needed.

MicroRNAs (miRNAs) are highly conserved non-coding RNAs that inhibit translation and cleave mRNAs by base pairing with the 3' untranslated region (UTR) of target genes, thereby regulating various biological processes [4] [5]. Research has demonstrated that epigenetics significantly contributes to the pathogenesis of osteosarcoma (OS), with miRNAs, as members of the non-coding RNA family, playing a crucial role in the regulation of post-transcriptional gene expression [6]. Although miR-30b-5p has been implicated in the regulation of malignant tumor progression, the precise mechanism by which it influences the malignant phenotype of osteosarcoma remains to be elucidated [7]. In this study, we upregulated the expression of miR-30b-5p in osteosarcoma cells and assessed the resulting changes in cell proliferation, invasion, migration, and apoptosis. Additionally, we evaluated the expression levels of P4HA2 and apoptosis-related proteins to elucidate the specific mechanisms by which miR-30b-5p influences the malignant phenotype of osteosarcoma cells. This research aims to provide insights and identify new targets for therapeutic strategies in osteosarcoma.

2. Materials and Methods

The human osteosarcoma MG63 cell line was obtained from Wuhan Prosperity Biotechnology Co., Ltd. Fetal bovine serum was also sourced from this company. RPMI-1640 culture medium was purchased from HyClone, USA. Lipofectamine 3000 was acquired from Invitrogen, USA. The RNA extraction kit, reverse transcription kit, and RT-PCR reagents were obtained from TaKaRa, Japan. Additionally, the CCK8 assay kit, Annexin V-FITC apoptosis detection kit, BCA protein

quantification kit, RIPA protein lysate, and SDS-PAGE gel were also sourced from TaKaRa, Japan. The CCK8 test kit, Annexin V-FITC apoptosis detection kit, BCA protein quantification kit, RIPA protein lysate, and SDS-PAGE gel preparation kit were purchased from Shanghai Biyuntian Biotechnology Co. Abclonal. GAPDH was acquired from Pro-Tech Biotechnology. The miR-30b-5p mimics (mimics), negative control (miR-NC), and related primers were synthesized by Starfish Bioengineering Co.

2.1. Experimental Methods

2.1.1. Cell Culture and Transfection

The osteosarcoma MG63 cells were cultured in RPMI-1640 medium supplemented with 10% fetal bovine serum in an incubator maintained at 37˚C with 5% CO^2. The experiment comprised a negative control group and a mimics treatment group, with MG63 cells transfected using liposome-encapsulated miR-NC and miR-30b-5p mimics, respectively. Cells were collected 48 hours post-transfection for subsequent experiments. The procedure is summarized as follows: logarithmically growing MG63 cells were inoculated at a density of 1×10^5 cells per well in a 6-well plate. Once the cell confluence reached approximately 70%, the original medium was discarded, and fresh serum-free medium was added. miR RNA was diluted with Lipofectamine 3000 transfection reagent in 500 μL of serum-free medium, mixed thoroughly, and then incubated with the cells for 20 minutes at room temperature before being added to the culture wells. Following this incubation, the culture medium was replaced with RPMI-1640 medium containing 10% fetal bovine serum, and the cells were further incubated.

2.1.2. CCK8 Assay to Detect Cell Proliferation

The resuspended cells were collected and diluted with 200 μL of growth medium before being inoculated into 96-well plates at a density of 1×10^5 cells per well, with five replicate wells for each group. The cells were cultured for 24, 48, and 72 hours for subsequent CCK8 detection. The CCK8 assay involved adding 100 μL of diluted CCK8 assay solution to each well, followed by an 80-minute incubation period. The optical density (OD) at 450 nm was measured, and the final optical density value was calculated by subtracting the blank well values from the measured values. Wells containing only the CCK8 assay solution served as blank control wells, with the assay solution diluted in a 1:9 ratio with growth medium.

2.1.3. Transwell Assay Detects Cell Invasion Ability

Matrigel matrix stored at −80˚C was thawed overnight at 4˚C until it liquefied. Subsequently, 50 μL of the matrix gel was added to each Transwell and incubated for 30 minutes in a standard incubator. The cell culture medium in each group was completely removed, cells were washed twice with PBS, and then digested with trypsin-EDTA. The digestion was halted by adding complete culture medium and gently mixing the cells. Subsequently, 10^4 cells were transferred to 1.5 mL EP tubes, centrifuged at 1000 rpm for 5 minutes, the supernatant was discarded, and

the cells were resuspended in 200 μL of serum-free medium before being added to the Transwell. The lower chamber was filled with 1 mL of medium, and the Transwell was incubated at 37˚C for 24 hours. After incubation, the Transwell was removed, cells on the upper side were wiped off with a cotton swab, and the remaining cells were gently washed with PBS. Cells on the underside of the Transwell were fixed with 4% paraformaldehyde for 30 minutes, followed by staining with crystal violet solution for 15 minutes. The membrane was rinsed, mounted on a slide, and examined. Finally, the stained cells were imaged using an inverted microscope at 200× magnification.

2.1.4. Transwell Assay to Detect Cell Migration Ability

Discard the cell culture medium from each group and wash the cells twice with PBS. Add trypsin-EDTA solution for digestion, then terminate the digestion by adding complete culture medium and gently mixing the cells. Transfer 10^4 cells into 1.5 mL EP tubes and centrifuge at 1000 rpm for 5 minutes. Remove the supernatant, resuspend the cells in 200 μL of serum-free medium, and introduce them into the Transwell. Add 1 mL of medium to the lower chamber and incubate at 37˚C for 24 hours. After incubation, remove the Transwell, wipe the cells from the upper surface with a cotton swab, and gently wash any remaining cells with PBS. Fix the cells on the reverse side of the Transwell with 4% paraformaldehyde for 30 minutes, then immerse them in crystal violet staining solution for 15 minutes. Wash the membrane and mount it on a slide for observation. Finally, photograph the stained cells using an inverted microscope at 200× magnification.

2.1.5. Detection of Apoptosis by Flow Cytometry

Cells from each group were individually collected with three replicates per group, and apoptosis was assessed following the AnnexinV-FITC/PI kit protocol. The experimental procedure involved washing cells with 1 × PBS, pelleting cells by centrifugation, resuspending them in 500 μL of PBS, incubating the cells in each group successively with 10 μL of AnnexinV-FITC at room temperature in the dark for 15 minutes, followed by 5 μL of PI at room temperature in the dark for 5 minutes. Subsequently, apoptosis levels in each group were determined and analyzed using BD flow cytometry.

2.1.6. Dual Luciferase Activity Assay

The direct interaction between miRNA-30b-5p and the 3' UTR of P4HA2 was confirmed through a dual luciferase reporter gene assay. The primary steps of this assay are outlined as follows: cell suspensions were prepared from logarithmically growing cells and seeded into 24-well plates. Once the cell confluence reached approximately 60%, transfection was performed using Lipofectamine 3000 transfection reagent according to the following group assignments: Group A was transfected with miRNA-30b-5p mimics and the wild-type (WT) plasmid containing the P4HA2 3'-UTR; Group B received miRNA-negative control (NC) and the WT plasmid; Group C was transfected with miRNA-30b-5p mimics and the mutant (MUT) plasmid containing the P4HA2 3'-UTR; and Group D was transfected with

miRNA-NC and the MUT plasmid. After 48 hours of transfection, the relative luciferase activity levels among the different groups were measured using the dual luciferase assay system.

2.1.7. RNA Extraction and RT-PCR for Detection of mRNA Expression of Target Molecules

Total RNA was extracted from MG63 cell lines or osteosarcoma (OS) tissues utilizing TRIzol reagent, and RNA content was quantified via UV spectrophotometry. cDNA synthesis from the extracted total RNA was conducted using a reverse transcription kit, followed by PCR reactions performed in accordance with the provided instructions. The expression level of miR-30b-5p was assessed with U6 serving as an internal reference, while the expression level of P4HA2 was measured using GAPDH as an internal reference.

2.1.8. Protein Extraction and Western Blot Assay for Protein Expression of Target Molecules

Each group of cells was collected separately, and total protein was extracted from each group following the instructions provided in the BCA Protein Extraction Kit. After quantifying the protein, 20 μg from each group was separated using SDS-PAGE gel electrophoresis. Subsequently, the proteins were transferred to a PVDF membrane, which was blocked with 5% skimmed milk powder at room temperature for 1 hour. The primary antibody was then incubated at 4˚C overnight, followed by washing with TBST. The secondary antibody was hybridized for 1 hour, and chemiluminescence was developed using ECL substrate. The antibodies utilized included P4HA2 monoclonal rabbit antibody (1:1100 dilution), BAX monoclonal rabbit antibody (1:800 dilution), BCL-2 monoclonal rabbit antibody (1:1000 dilution), and GAPDH monoclonal mouse antibody (1:10,000 dilution).

2.2. Statistical Methods

Statistical analysis was conducted using GraphPad Prism version 10.6.0. Data are presented as mean ± standard deviation (± s). A t-test was employed to compare the two groups, with a significance threshold set at $P < 0.05$.

3. Results

3.1. miR-30b-5p Mimics Transfection-Mediated Changes in miR-30b-5p Expression Levels

MG63 osteosarcoma cells were transfected with either miR-NC control or miR-30b-5p mimics, and the expression levels of miR-30b-5p were assessed using RT-PCR. The results indicated that the expression of miR-30b-5p was significantly elevated in the miR-30b-5p mimics-treated group compared to the miR-NC group, with relative expression levels of 1.008 ± 0.093 versus 312.1 ± 4.0, respectively ($t = 77.53$, $p = 0.0002$, **Figure 1**). These findings confirm the successful establishment of a miR-30b-5p overexpression system in MG63 osteosarcoma cells. This overexpression cell model can be utilized for subsequent studies on the ma-

lignant phenotypes of osteosarcoma.

3.2. Effect of miR-30b-5p Overexpression on Cell Proliferation Detected by CCK8 Assay

MG63 osteosarcoma cells were transfected with miR-NC control and miR-30b-5p mimics for durations of 12 h, 24 h, 48 h, and 72 h, after which their proliferative abilities were assessed using the CCK8 assay. The results indicated that the proliferation of cells in the miR-30b-5p mimics group was significantly inhibited compared to the miR-NC group (Figure 2). At the 24 h mark, the proliferative capacities of the miR-NC and miR-30b-5p mimics groups were (144.9 ± 7.2)% and (88.4 ± 3.4)%, respectively ($t = 16$, $P < 0.001$). After 48 h of transfection, the proliferative capacities of the two groups were (179.3 ± 11.2)% for miR-NC and (112.4 ± 5.8)% for miR-30b-5p mimics ($t = 5.318$, $P < 0.0001$). At the 72 h time point, the proliferative capacity of the miR-NC group was (311.4 ± 17.8)% compared to (178.2

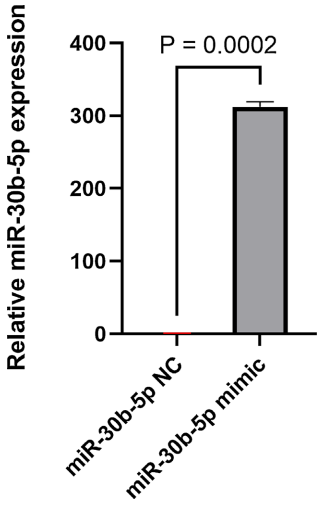

Figure 1. The expression of miR-30b-5p in MG63 cells after transfection.

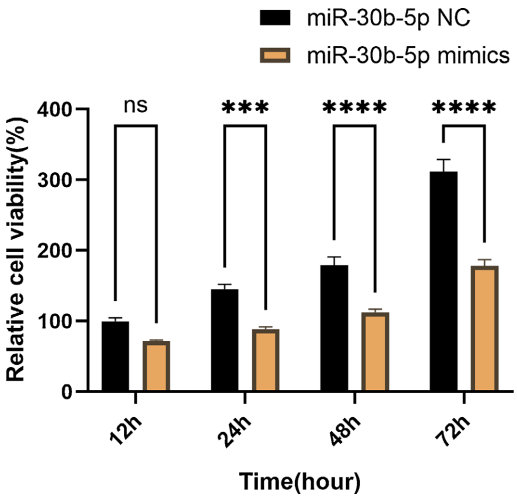

Figure 2. The effect of miR-30b-5p on the proliferation of MG63 cells (ns $P > 0.05$; **$P < 0.01$; ****$P < 0.0001$).

± 9.9)% for the miR-30b-5p mimics group (t = 10.58, P < 0.0001). These findings demonstrate that high expression of miR-30b-5p significantly inhibits the proliferation of MG63 osteosarcoma cells.

3.3. Transwell Assay to Detect the Effect of miR-30b-5p Overexpression on Cell Invasion Ability

MG63 osteosarcoma cells were transfected with either miR-NC or miR-30b-5p mimics, and the subsequent effect of miR-30b-5p on the invasive capacity of the cells was assessed using a Transwell assay. The results indicated a significant reduction in cell invasion ability in the miR-30b-5p mimics-treated group compared to the miR-NC group. The cell counts for the miR-NC group were 158.6 ± 9.4 and 58.7 ± 5.6, respectively, while those for the miR-30b-5p mimics group were significantly lower (t = 8.92, P < 0.0001). This finding suggests that high expression of miR-30b-5p markedly inhibits the invasive ability of MG63 osteosarcoma cells (Figure 3).

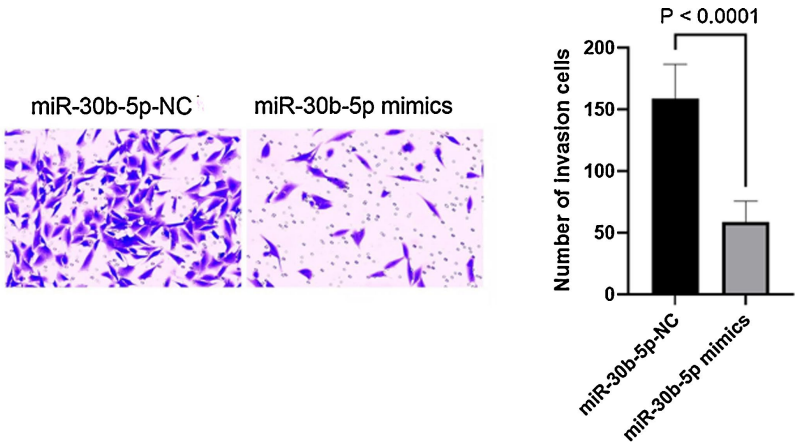

Figure 3. Effect of miR-30b-5p on the invasive ability of MG63 by Transwell (crystal violet staining ×200).

3.4. Transwell Assay to Detect the Effect of miR-30b-5p Overexpression on Cell Migration Ability

MG63 osteosarcoma cells underwent transfection with miR-NC and miR-30b-5p mimics, and the impact of miR-30b-5p on cell migration was assessed using a Transwell assay. The findings indicated a significant decrease in migration ability among cells in the miR-30b-5p mimics group compared to those in the miR-NC group. Cell counting from the Transwell assay demonstrated a notable disparity in cell numbers between the miR-NC group (207.1 ± 7.2) and the miR-30b-5p mimics group (93.0 ± 4.2) (t = 23, P < 0.0001), implying the inhibitory effect of miR-30b-5p on MG63 osteosarcoma cell migration (Figure 4).

3.5. Effect of miR-30b-5p Overexpression on Apoptosis Detected by Flow Cytometry

MG63 osteosarcoma cells were transfected with miR-NC and miR-30b-5p mim-

ics, and subsequent changes in apoptosis levels were assessed using flow cytometry. The results revealed that the percentage of apoptosis in the miR-NC group was 3.2 ± 1.0%, while the miR-30b-5p mimics group exhibited a significantly higher rate of 33.7 ± 1.9% (t = 14.06, P = 0.0001). These findings indicate that miR-30b-5p markedly enhances apoptosis levels in MG63 osteosarcoma cells (Figure 5).

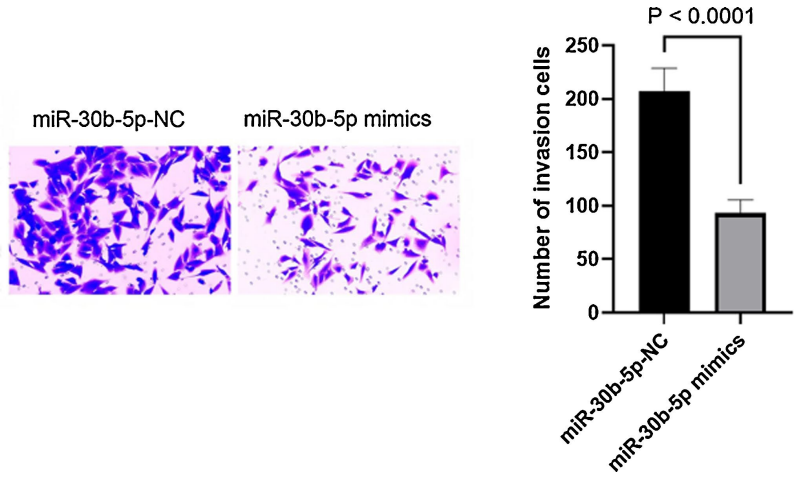

Figure 4. Effect of miR-30b-5p on the migratory ability of MG63 by Transwell (crystal violet staining ×200).

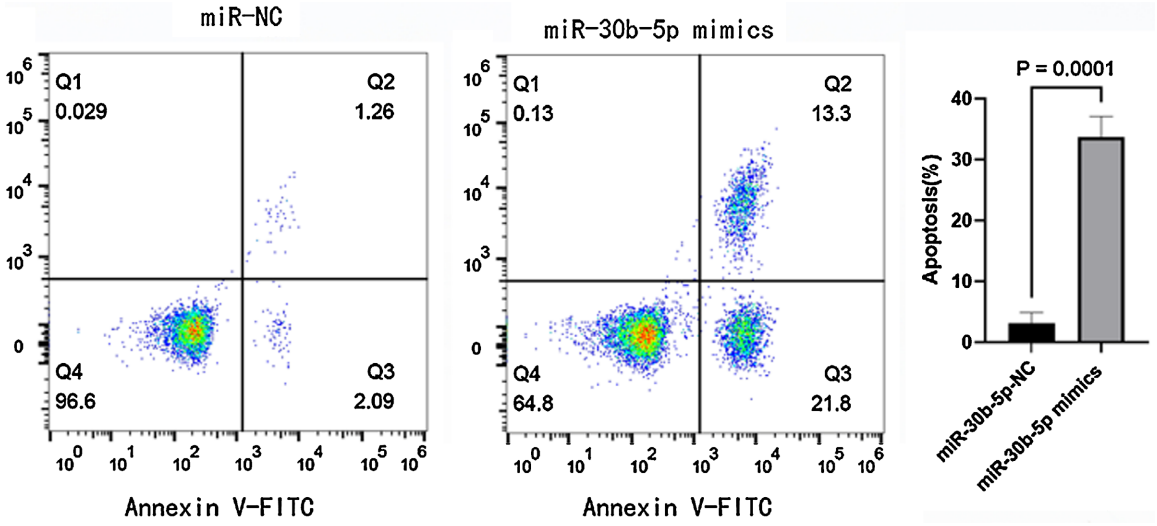

Figure 5. Effect of miR-30b-5p on apoptosis of MG63 by flow cytometry.

3.6. Targeted Regulation of P4HA2 by miR-30b-5p as Detected by Dual Luciferase Activity

To validate the downstream molecules targeted and regulated by miR-30b-5p in MG63 osteosarcoma cells, P4HA2 was identified as a potential downstream target through bioinformatics predictions and literature review. Analysis using the TargetScan database indicated that the 3'-UTR sequence of P4HA2 is partially complementary to miR-30b-5p (Figure 6(a)). Based on this prediction, wild-type

(WT) and mutant (MUT) plasmids containing the P4HA2 3'-UTR were co-transfected with either miR-NC or miR-30b-5p mimics in MG63 cells. The luciferase activities of these four groups were subsequently measured separately. The results demonstrated that the luciferase activity of the miR-30b-5p mimics was significantly inhibited following co-transfection with the wild-type plasmid containing the P4HA2 3'-UTR (Figure 6(b)). The viability of the miR-NC co-transfected with the wild-type plasmid containing the P4HA2 3'-UTR was recorded at 1.0% and 1.0%, respectively. In contrast, the viability of the mimics was measured at 1.000 ± 0.032 and 0.504 ± 0.032 ($t = 10.87$, $P < 0.0001$), indicating that miR-30b-5p can inhibit the expression of P4HA2 3'-UTR by directly interacting with it. Thus, P4HA2 is confirmed as a direct target molecule of miR-30b-5p.

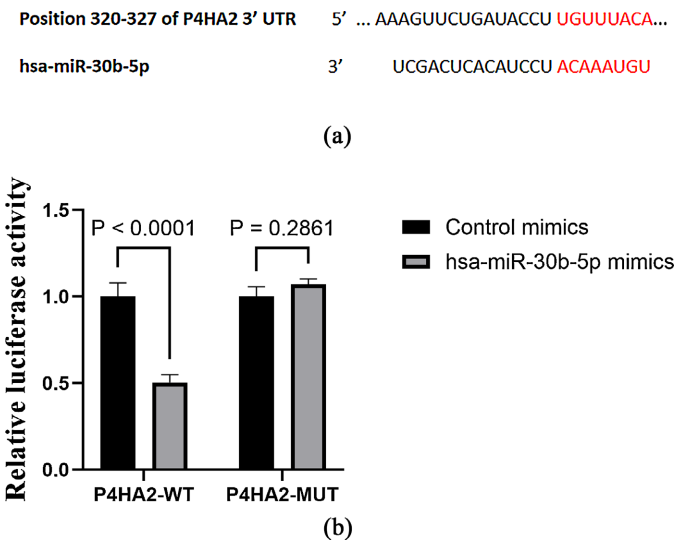

Figure 6. Targeted regulation of P4HA2 by miR-30b-5p through dual luciferase reporter assay ((a) The binding site of P4HA2 and miR-30b-5p; (b) Detection of luciferase activity).

3.7. Effect of miR-30b-5p Overexpression on mRNA Expression of P4HA2 in Osteosarcoma Cells Detected by RT-PCR

MG63 osteosarcoma cells were transfected with either miR-NC or miR-30b-5p mimics, and the mRNA expression level of P4HA2 in these cells was assessed using RT-PCR. The results indicated that miR-30b-5p mimics significantly inhibited P4HA2 expression in MG63 cells. Specifically, the mRNA expression levels of P4HA2 in the miR-NC and miR-30b-5p mimics groups were 1.008 ± 0.053 and 0.171 ± 0.031, respectively ($t = 9.093$, $P = 0.0114$, Figure 7).

3.8. Effect of miR-30b-5p Overexpression on the Expression of P4HA2 and Apoptosis-Related proteins in Osteosarcoma Cells Detected by Western Blot

MG63 osteosarcoma cells were treated with miR-NC and miR-30b-5p mimics, and the effects of miR-30b-5p mimics on the expression of P4HA2 and apoptosis-related proteins BAX and BCL-2 were assessed using Western blot analysis. The

results indicated that the expression of P4HA2 and the anti-apoptotic protein BCL-2 decreased in the miR-30b-5p mimics group. In contrast, the expression of the apoptosis-promoting protein BAX significantly increased in MG63 cells compared to the miR-NC group. These findings suggest that miR-30b-5p inhibits the expression of P4HA2 and concurrently regulates various apoptosis-related proteins, thereby promoting the apoptosis of osteosarcoma cells (Figure 4, Figure 8).

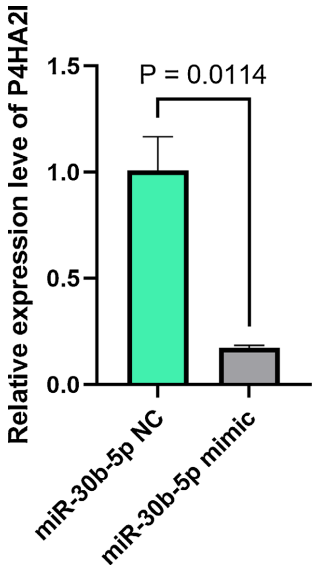

Figure 7. The effect of miR-30b-5p on the expression of P4HA2 mRNA in MG63 cells.

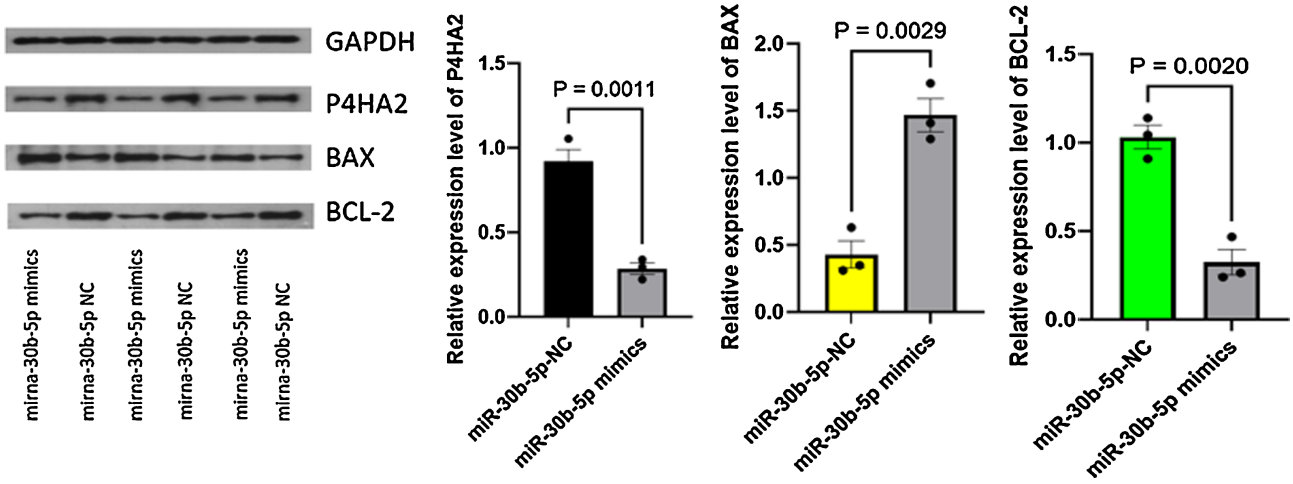

Figure 8. The effect of miR-30b-5p on the expression of P4HA2 and apoptosis-related proteins in MG63 cells

4. Discussion

Osteosarcoma represents the most prevalent primary malignant bone tumor, primarily affecting children and adolescents [1]. Despite its rarity, osteosarcoma is associated with high rates of disability and mortality. The annual incidence rate is approximately 3% - 5% [8]. Recent advancements in the treatment of osteosarcoma encompass stem cell therapy, immunotherapy, and gene therapy [9] [10].

Over the decades, multidrug chemotherapy has improved the 5-year survival rate for localized osteosarcoma from less than 20% to around 60%. Consequently, the development of innovative strategies for the early diagnosis and treatment of osteosarcoma patients is essential. The gene p4HA2 has been identified as a partial epithelial-mesenchymal transition (EMT)-related gene, with its overexpression significantly correlating with poor prognosis in patients with hepatocellular carcinoma (HCC) [11]. MicroRNAs (miRNAs) regulate various biological processes, including cell differentiation, metastasis, apoptosis, and proliferation, and play a role in the pathogenesis of numerous tumors [12]. In this study, we investigated the impact of miR-30b-5p on the malignant phenotype of osteosarcoma and its specific molecular mechanisms.

Several studies have established the role of miRNA-30b in the carcinogenesis and progression of osteosarcoma [7]. miRNA-30b-5p has been linked to cancer development and progression across various malignancies, including renal cell carcinoma [13], breast cancer [14], and pancreatic cancer [15]. In this study, the expression of miR-30b-5p was significantly upregulated in osteosarcoma MG63 cells transfected with miR-30b-5p mimics, indicating high transfection efficiency. The activity and proliferation of MG63 cells transfected with miR-30b-5p mimics were significantly lower than those of control cells, suggesting that miR-30b-5p plays a role in inhibiting MG63 cell proliferation, with this tumor-suppressive effect manifesting early during the transfection process. The upregulation of miR-30b-5p expression in this study demonstrated that the invasion and migration capabilities of MG63 cells were significantly inhibited, indicating the inhibitory effect of miR-30b-5p on distal metastasis in MG63 cells. To assess the impact of miR-30b-5p on various malignant phenotypes of osteosarcoma cells, the study also evaluated changes in apoptosis levels of MG63 cells. It was observed that elevated expression of miR-30b-5p significantly enhanced apoptosis levels. Furthermore, miR-30b-5p mediated the upregulation of the pro-apoptotic protein BAX and the downregulation of the anti-apoptotic protein BCL-2. These findings confirm the role of miR-30b-5p in inhibiting the malignant phenotype of osteosarcoma cells.

To further elucidate the molecular mechanism underlying miR-30b-5p inhibition in osteosarcoma, survival analysis indicated that elevated expression of P4HA2 correlated with poor overall survival (OS) in osteosarcoma patients, and P4HA2 demonstrated strong predictive capability for OS [16]. To determine whether miR-30b-5p influences the malignant phenotype of osteosarcoma through targeting P4HA2, bioinformatics predictions were conducted utilizing the TargetScan database. Biosignature analysis revealed that the 3'-UTR sequence of P4HA2 exhibited partial complementarity to miR-30b-5p, a finding that was subsequently validated using a dual luciferase reporter system. It was established that miR-30b-5p downregulated P4HA2 expression by interacting with its 3'-UTR, thereby confirming that P4HA2 is a downstream target molecule positively regulated by miR-30b-5p.

The experimental results indicate that miR-30b-5p can inhibit the proliferation,

invasion, and migration of osteosarcoma cells while promoting apoptosis. This effect may be linked to the targeted down-regulation of P4HA2 expression. Furthermore, modulation of miR-30b-5p appears to concurrently influence P4HA2 protein levels and cellular phenotype, establishing a comprehensive chain of evidence for this correlation. However, from a rigorous mechanistic standpoint, the current experimental design requires an essential step to definitively establish the causal relationship that "miR-30b-5p exerts its tumor suppressor function through down-regulation of P4HA2". Specifically, we have yet to provide the most direct evidence through "functional recovery experiments". Ideally, the design should involve restoring P4HA2 expression in cells with miR-30b-5p overexpression-induced phenotypic inhibition, thereby removing the regulation by miR-30b-5p, and observing whether the inhibited proliferation and invasion phenotypes can be partially or completely "rescued". Conversely, P4HA2 should be knocked down in cells suppressed by miR-30b-5p to determine whether the enhancement of phenotypes is obstructed. Future studies that incorporate this level of validation will be able to conclusively eliminate the possibility that miR-30b-5p acts through alternative targets, thereby providing irrefutable causal evidence for the pivotal role of the miR-30b-5p/P4HA2 axis in osteosarcoma.

5. Conclusion

The findings of this study indicate that miR-30b-5p in the MG63 osteosarcoma cell line plays a role in inhibiting the proliferation, invasion, and migration of osteosarcoma cells, as well as in inducing apoptosis by targeting and down-regulating the expression of P4HA2. This discovery offers a novel target and potential therapeutic strategy for the treatment of osteosarcoma. The conclusions of this study primarily derive from experimental analyses conducted on the osteosarcoma MG63 cell line. While this approach offers valuable foundational data for elucidating the biological role of the miR-30b-5p/P4HA2 axis, a notable limitation is the exclusive use of a single cell line. Osteosarcoma exhibits significant intratumoral and intertumoral heterogeneity, resulting in variations in genetic backgrounds and phenotypes among different cell lines. Consequently, future research should aim to replicate the validation of key experiments and perform complementary functional restoration experiments using additional representative osteosarcoma cell lines, such as U2-OS, Saos-2, or 143B, to enhance the generalizability and reliability of the study's findings.

Data Availability

The datasets generated or analyzed in the current study will be available upon reasonable request.

Funding

1) Joint Special Project of Guangxi Natural Science Foundation (2025GXNSFHA069021).

2) Guangxi Medical and Health Appropriate Technology Development and Promotion Project (S2022139).
3) Basic and Clinical Research on Degenerative Diseases of Bones and Joints (Right Medical University Affiliated Hospital Document No. 57 [2023]).

Authors' Contributions

W L and W F contributed to the study design and data acquisition, drafted the manuscript, and were the co-first authors. T S and W T contributed to contributed experimental data. C L was considered the co-correspondence author. All authors have read and approved the final manuscript.

Conflicts of Interest

The authors declare no conflicts of interest regarding the publication of this paper.

References

[1] Beird, H.C., Bielack, S.S., Flanagan, A.M., Gill, J., Heymann, D., Janeway, K.A., *et al.* (2022) Osteosarcoma. *Nature Reviews Disease Primers*, **8**, Article No. 77. https://doi.org/10.1038/s41572-022-00409-y

[2] Tian, H., Cao, J., Li, B., Nice, E.C., Mao, H., Zhang, Y., *et al.* (2023) Managing the Immune Microenvironment of Osteosarcoma: The Outlook for Osteosarcoma Treatment. *Bone Research*, **11**, 1 Article No. 1. https://doi.org/10.1038/s41413-023-00246-z

[3] Lei, T., Qian, H., Lei, P. and Hu, Y. (2021) Ferroptosis-Related Gene Signature Associates with Immunity and Predicts Prognosis Accurately in Patients with Osteosarcoma. *Cancer Science*, **112**, 4785-4798. https://doi.org/10.1111/cas.15131

[4] He, B., Zhao, Z., Cai, Q., Zhang, Y., Zhang, P., Shi, S., *et al.* (2020) miRNA-Based Biomarkers, Therapies, and Resistance in Cancer. *International Journal of Biological Sciences*, **16**, 2628-2647. https://doi.org/10.7150/ijbs.47203

[5] Menon, A., Abd-Aziz, N., Khalid, K., Poh, C.L. and Naidu, R. (2022) miRNA: A Promising Therapeutic Target in Cancer. *International Journal of Molecular Sciences*, **23**, Article No. 11502. https://doi.org/10.3390/ijms231911502

[6] Wang, J., Pang, W., Zuo, Z., Zhang, W. and He, W. (2017) MicroRNA-520b Suppresses Proliferation, Migration, and Invasion of Spinal Osteosarcoma Cells via Downregulation of Frizzled-8. *Oncology Research Featuring Preclinical and Clinical Cancer Therapeutics*, **25**, 1297-1304. https://doi.org/10.3727/096504017x14873430389189

[7] Xu, Y., Yao, T., Huang, K., Liu, G., Huang, Y., Gao, J., *et al.* (2020) Circular RNA circTUBGCP3 Is Up-Regulated and Promotes Cell Proliferation, Migration and Survivability via Sponge MiR-30b in Osteosarcoma. *OncoTargets and Therapy*, **13**, 3729-3737. https://doi.org/10.2147/ott.s245366

[8] Zhou, Y., Yang, D., Yang, Q., Lv, X., Huang, W., Zhou, Z., *et al.* (2020) Single-Cell RNA Landscape of Intratumoral Heterogeneity and Immunosuppressive Microenvironment in Advanced Osteosarcoma. *Nature Communications*, **11**, Article No. 6322. https://doi.org/10.1038/s41467-020-20059-6

[9] Gill, J. and Gorlick, R. (2021) Advancing Therapy for Osteosarcoma. *Nature Reviews Clinical Oncology*, **18**, 609-624. https://doi.org/10.1038/s41571-021-00519-8

[10] Huang, Q., Liang, X., Ren, T., Huang, Y., Zhang, H., Yu, Y., *et al.* (2021) The Role of Tumor-Associated Macrophages in Osteosarcoma Progression—Therapeutic Implications. *Cellular Oncology*, **44**, 525-539. https://doi.org/10.1007/s13402-021-00598-w

[11] Lei, Y., Yan, W., Lin, Z., Liu, J., Tian, D. and Han, P. (2020) Comprehensive Analysis of Partial Epithelial Mesenchymal Transition-Related Genes in Hepatocellular Carcinoma. *Journal of Cellular and Molecular Medicine*, **25**, 448-462. https://doi.org/10.1111/jcmm.16099

[12] Lai, X., Schmitz, U. and Vera, J. (2022) The Role of MicroRNAs in Cancer Biology and Therapy from a Systems Biology Perspective. In: *Advances in Experimental Medicine and Biology*, Springer International Publishing, 1-22. https://doi.org/10.1007/978-3-031-08356-3_1

[13] Xie, M., Lv, Y., Liu, Z., Zhang, J., Liang, C., Liao, X., *et al.* (2018) Identification and Validation of a Four-miRNA (miRNA-21-5p, miRNA-9-5p, miR-149-5p, and miRNA-30b-5p) Prognosis Signature in Clear Cell Renal Cell Carcinoma. *Cancer Management and Research*, **10**, 5759-5766. https://doi.org/10.2147/cmar.s187109

[14] Estevão-Pereira, H., Lobo, J., Salta, S., Amorim, M., Lopes, P., Cantante, M., *et al.* (2019) Overexpression of Circulating MiR-30b-5p Identifies Advanced Breast Cancer. *Journal of Translational Medicine*, **17**, Article No. 435. https://doi.org/10.1186/s12967-019-02193-y

[15] Chen, K., Wang, Q., Liu, X., Wang, F., Yang, Y. and Tian, X. (2022) Hypoxic Pancreatic Cancer Derived Exosomal miR-30b-5p Promotes Tumor Angiogenesis by Inhibiting GJA1 Expression. *International Journal of Biological Sciences*, **18**, 1220-1237. https://doi.org/10.7150/ijbs.67675

[16] Chen, H., Han, X., Sun, H., Xie, T. and Fan, X. (2024) Genomic Nursing Science Revealed the Prolyl 4-Hydroxylase Subunit Alpha 2 as a Significant Biomarker Involved in Osteosarcoma. *Heliyon*, **10**, e27191. https://doi.org/10.1016/j.heliyon.2024.e27191